Journal of Power Sources 254 (2014) 183–189

Contents lists available at ScienceDirect

Journal of Power Sources

journal homepage: www.elsevier.com/locate/jpowsour

Preparation and characterizations of highly dispersed carbon supported Pd_xPt_y/C catalysts by a modified citrate reduction method for formic acid electrooxidation

Zuopeng Li [a], Muwu Li [b], Mingjia Han [b], Jianhuang Zeng [b,*], Yuexia Li [c], Yanqin Guo [b], Shijun Liao [b]

[a] Institute of Applied Chemistry, Shanxi Datong University, No. 5 Xingyun Street, Datong 037009, China
[b] School of Chemistry and Chemical Engineering, South China University of Technology, Guangdong Key Lab for Fuel Cell Technology, Guangzhou 510641, China
[c] North University of China, Shuozhou, No. 65 Changning Street, Shuozhou 036000, China

HIGHLIGHTS

- Pd_xPt_y/C with an average particle size of 3 nm were prepared by a citrate reduction method with KNO_3.
- CO striping and repeated CV were used to test the CO tolerance and stability respectively.
- The catalysts' mass activity for formic acid oxidation outperformed those from literature.

ARTICLE INFO

Article history:
Received 23 October 2013
Received in revised form
9 December 2013
Accepted 30 December 2013
Available online 8 January 2014

Keywords:
Citrate reduction
PtPd catalysts
Catalysts segregation
Formic acid oxidation

ABSTRACT

Carbon supported Pd_xPt_y/C (atomic ratio *x*:*y* from 1:1 to 6:1) have been prepared by a modified citrate reduction method assisted by inorganic stabilizers. Without using high molecular capping agents as stabilizers, the Pd_xPt_y/C catalysts are highly dispersed on the carbon support and no particle aggregations are found for the Pd_xPt_y/C catalysts. X-ray photoelectron spectroscopy reveals either Pt or Pd segregation for the Pd_xPt_y/C catalysts depending on Pd/Pt atomic ratio. CO stripping in 0.5 M H_2SO_4 and repeated formic acid oxidation cyclic voltammetry in 0.5 M HCHO + 0.5 M H_2SO_4 have been conducted to test out the CO tolerance and stability of the catalysts, respectively. It has been found that, with the increase of Pd/Pt atomic ratio, the CO stripping peak potential increases (less CO tolerant), whereas the catalyst stability towards formic acid oxidation decreases. The as-prepared catalysts reveal excellent mass-normalized formic acid oxidation activity as compared with published results possibly due to high dispersion and the absence of high molecular capping agents.

1. Introduction

In applications for portable power devices, polymer electrolyte membrane fuel cells (PEMFC) are generally thought of as promising candidates to replace Lithium ion batteries [1–4]. Although H_2-powered fuel cells have been the dominant choices in PEMFCs, they still suffer a series of limitations such as the cost of the electrocatalysts "mainly Pt", the public concerns on the hydrogen safety and their low energy density. Second to H_2-powered fuel cell, direct methanol fuel cell (DMFC) has an impressively high energy density (4690 Wh l^{-1}) since it uses liquid method as fuel, but its anodic methanol electrocatalytic oxidation rate is very low relative to that of H_2. In addition, due to limited methanol compatibility with Nafion membranes, only low fuel concentrations are allowed to feed to a DMFC [5,6]. Alternative to DMFC, direct formic acid fuel cell (DFAFC) has a higher electromotive force (open circuit potential ~1.48 V) and runs on formic acid, a liquid generally recognized as safe at room temperature [7]. And what's more, formic acid has a smaller crossover flux through Nafion relative to methanol, which allows for the use of higher fuel concentrations and thinner membranes in DFAFCs [8].

There are two most commonly recognized formic acid oxidation mechanisms, one proceeds via the so-called "parallel or dual pathway" in which weakly adsorbed CO intermediates are formed, whereas the direct oxidation pathway mechanism occurs through a direct dehydrogenation reaction with CO_2 as final products [9].

* Corresponding author. Tel.: +86 20 39099665.
E-mail address: cejhzeng@scut.edu.cn (J. Zeng).

0378-7753/$ – see front matter © 2014 Elsevier B.V. All rights reserved.
http://dx.doi.org/10.1016/j.jpowsour.2013.12.118

Electrooxidation of formic acid is usually catalysed by carbon supported Pt or Pt based catalysts [10]. However, the direct formic acid fuel cell performance incorporating Pt catalysts is not satisfied due to notable CO poisoning (parallel pathway mechanism) on Pt [8,11–16]. Intensive attentions nowadays have been paid to Pd or Pd based catalysts for formic acid oxidation since the electrochemical oxidation of formic acid on Pd produces carbon dioxide directly, without forming adsorbed CO intermediates [17]. Although the cell performance operated on Pd catalysts is better than that on Pt catalysts, the former suffers steady degradation in prolonged potential cycling due to Pd dissolution in acidic solutions [18]. Therefore, DFAFCs run on Pt or Pd alone catalysts either have high performance and short longevity or *vice versa*. Combining the merits of Pt and Pd to form carbon supported Pd_xPt_y catalysts seems to be a promising outlet for better addressing the concurrent issues of degradation and CO poisoning [5,11,12,19–21].

In order to obtain Pd_xPt_y catalysts with high activity, addition of high molecular capping agents for fine dispersion was a conventional practice in the published references. For example, carbon supported Pd_xPt_{1-x} catalysts were synthesized by a modified polyol process with poly(*N*-vinyl-2-pyrrolidone) (PVP) as a stabilizer by Baranova et al. [12] and it was found that 4 nm sized $Pd_{0.5}Pt_{0.5}$ exhibited improved steady state activity for formic acid oxidation. Li and Hsing investigated Pt_xPd_{1-x} nanocatalysts for formic acid electrooxidation using 3-(*N*, *N*-dimethyldodecylammonio) propanesulfonate (SB12) as the stabilizer and methanol as the reducing agent, they found the co-deposition method was superior to the sequential-deposition one due to a possible synergistic effect between Pd and Pt [20]. Feng et al. also investigated the effect of deposition sequences on the electrocatalytic activity of PtPd/C for formic acid oxidation and found the catalytic activity and stability for Pt + Pd catalysts was greatly enhanced due to synergistic effects [19]. Pd_xPt_{1-x}/C catalysts were synthesized by a $NaBH_4$ reduction method stabilized by ethylenediaminetetraacetic acid (EDTA) and the $Pd_{0.9}Pt_{0.1}$/C catalyst was found to be the optimum catalyst due to inhibited CO poisoning at largely separated Pt sites [11]. In our previous work, we investigated the effects of Pd_xPt_y/C anode catalysts on the performance and stability of air breathing direct formic acid fuel cells [22]. The catalysts were prepared by the ethylene glycol method with large presence of citrate (molar ratio of citrate to metal precursor = 7.5:1) in order to obtain finely dispersed catalysts. The disadvantage of using high molecular stabilizers is the obvious obstacle of catalyst's active sites. Most recently, we developed a citrate reduction method assisted by inorganic salt stabilization to prepare Pt nanocatalysts for methanol oxidation [23]. The amount of citrate was minimized since the assisted stabilization of inorganic salt (KNO_3). In this work we prepared carbon-supported Pd and Pd_xPt_y anode catalysts by citrate reduction with the addition of KNO_3. Finely dispersed Pd_xPt_y/C catalysts were obtained with an average particle size of 3 nm via this method and the catalysts were intensively characterized by transmission electron microscopy and X-ray photoelectron spectroscopy for the catalytic oxidation of formic acid.

2. Experimental

Hydrogen hexachloroplatinum (IV) hydrate (H_2PtCl_6 $6H_2O$) and palladium chloride ($PdCl_2$) from Jinke Reagents (Shenyang, China), sodium citrate dehydrate (Na_3Cyt $2H_2O$), potassium nitrate (KNO_3), formic acid (88%, HCHO) and sulphuric acid (H_2SO_4) from Sinopharm Chemical Reagent, Nafion 117 solution (5 wt.% in a mixture of lower aliphatic alcohols and water) from Dupont, were used as received without further purification. De-ionized water processed by a Milli-Q water purification system was used throughout the investigation. Vulcan XC-72 carbon from Cabot was pretreated with acetone and a mixture of HNO_3+H_2O_2 followed with copious washing. The measured BET surface area for the processed carbon after vacuum drying was 225 m^2 g^{-1}. All glassware and Teflon-lined magnetic stirrers were cleaned with *aqua regia*, followed by copious rinsing with de-ionized water.

A typical synthesis for Pd_1Pt_1/C catalyst: 2.5 ml 0.0386 M H_2PtCl_6 (Pt 7.6 mg ml^{-1}) and 0.93 ml 0.1109 M $PdCl_2$ (Pd 11.8 mg ml^{-1}) aqueous solution was mixed with 7.7 ml 0.0386 M Na_3Cyt and 10.3 ml 0.386 M KNO_3 solution in a 500-ml flat-bottom flask and the content amounted to 400 ml with de-ionized water. A 10% KOH/H_2O solution was used to adjust the pH to be 10. The molar ratio of Na_3Cyt and KNO_3 to the total metal precursors (Pt^{4+} and Pt^{2+}) was kept at 1.5:1 and 15:1, respectively. The pretreated 120 mg Vulcan XC-72 was added to the above mixture with alternated magnetic stirring and ultrosonication until a homogeneous ink suspension was obtained. The XC-72 carbon added was calculated to collect 150 mg catalysts with a total metal loading of 20 wt.% in all the synthesis. The suspension mixture in the flask was then transferred into an oil bath and refluxed at 100 °C under magnetic stirring for 8 h. The suspension was then filtered to recover the solid, which was copiously washed with water before drying in vacuum at 70 °C overnight. Varying the molar ratio of Pd^{2+} and Pt^{4+} precursors would produce other Pd_xPt_y/C catalysts (where *x* and *y* represent molar ratio), i.e. Pd_2Pt_1/C, Pd_4Pt_1/C and Pd_6Pt_1/C. A 20 wt.% Pd/C and Pt/C was also prepared alongside for comparison.

Transmission electron microscopy (TEM) measurements were made on a FEI Tecnai G^2 F20 S-Twin with an accelerating voltage of 200 kV. The X-ray photoelectron spectroscopy (XPS) data were obtained with an AXIS Ultra DLD X-ray photoelectron spectrometer (Kratos, USA). The binding energies (BEs) were calibrated using the C 1s peak of graphite at 284.5 eV as the reference.

A conventional three-compartment electrochemical cell was used to evaluate the catalysts by cyclic voltammetry (CV). An Autolab PGSTAT302N served as the potentiostat/galvanostat. A rotating disk electrode (RDE, Pine Instrument Company, Model AFMSRCE) was used as the working electrode. The catalyst layer on the RDE was fabricated by casting 5 μl catalyst ink by micropipette (ink formation: 5 mg catalysts +1 ml 0.25 wt.% Nafion 117 (diluted by ethanol)) onto a 5 mm-diameter vitreous glassy carbon disk electrode. The total metal loading on the working electrode is 5 μg or 0.02551 mg cm^{-2}. A Pt wire and an Ag/AgCl in 3 M KCl were used as the counter and the reference electrodes, respectively, while 0.5 M HCHO in 0.5 M H_2SO_4 was the electrolyte for catalytic activity test. The electrochemically active surface area (ECSA) and CO stripping tests were performed in 0.5 M H_2SO_4 electrolyte. All reported potentials were referenced to Ag/AgCl in 3 M KCl. The catalysts were cycled between −0.1 V and 0.8 V at 20 mV s^{-1} until a stable response was obtained before cyclic voltammograms were recorded. The upper potential limit was set at 0.8 V for avoidance of Pd oxidation in high potentials. For CO stripping, a 10% CO in argon gas was employed. The electrolyte was saturated with the gas while the electrode was held at −0.1 V for 30 min. After CO adsorption, bulk CO was removed and the electrolyte was thoroughly purged by high purity Ar. CO stripping CV were collected from −0.1 V (starting potential) with two potential vertex at 0.8 V and −0.2 V. Completed oxidation of adsorbed species was accomplished in the first scan and no oxidation was found in the second scan. All electrochemical tests were recorded at room temperature.

3. Results and discussions

Citrate reduction of noble metal precursors are used for the preparation of Pd_xPt_y/C catalysts. The molar ratios of citrate to metal precursors are kept at 1.5:1 to reduce adverse capping agent

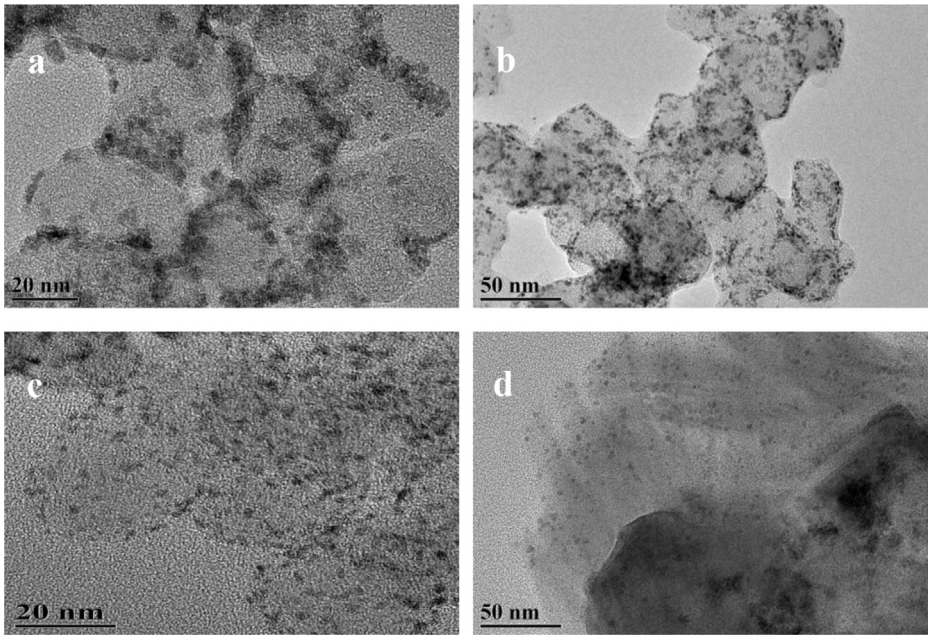

Fig. 1. TEM images for the catalysts of (a) Pd/C, (b, c) Pt/C and (c) Pd_2Pt_1/C.

effects on the catalyst activity. To improve the stability of nanoparticles, appropriate amount of KNO_3 was added. This method was found to be effective to produce finely dispersed nanoparticles in our latest work [23]. Fig. 1 shows the TEM images of the catalysts. Without addition of Pt, the carbon supported Pd alone catalyst (Fig. 1a) shows relatively poor dispersion. Aggregations of Pd nanoparticles are commonly seen and isolated Pd nanoparticles are rarely found. On the contrary, the Pt/C catalyst shows very good dispersion (Fig. 1b, c) without any appreciable particle agglomeration. The dispersion is better than that reported in Ref. [24] using the same citrate to platinum precursor atomic ratio but without use of inorganic salts. In comparison, the dispersion of Pd_2Pt_1/C catalyst in Fig. 1d (with an average particle size of 3 nm) was between that of Pd/C and Pt/C and the majority of noble metal nanoparticles are isolated without collision with each other. TEM images of the other Pd_xPt_y/C catalysts (not shown) also shows better dispersion which are probably contributed by the addition of Pt. It could be concluded that the addition of Pt to Pd improved the dispersion of nanoparticles, and this might contribute to the better stability of Pt nanoparticles relative to Pd.

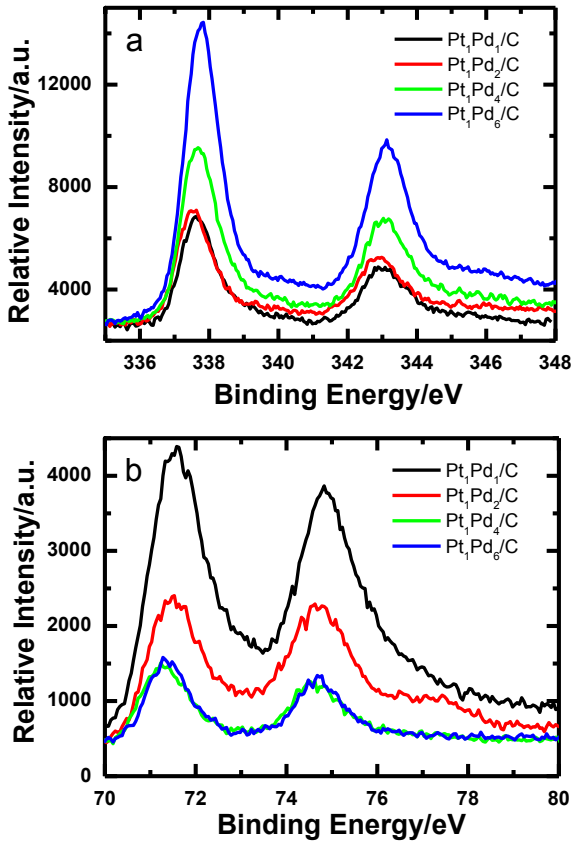

Fig. 2. XPS spectra for the catalysts (a) Pd 3d and (b) Pt 4f.

XPS analysis results indicated a fair agreement of nominal loading with the actual loading in the catalysts. The Pd 3d and Pt 4f spectra of the Pd_xPt_y/C catalysts are shown in Fig. 2a and b, respectively. The relative intensity increased expectedly with increasing Pd content in the following order: Pd_1Pt_1/C < Pd_2Pt_1/C < Pd_4Pt_1/C < Pd_6Pt_1/C (Fig. 2a), and *vice versa* the relative Pt intensity decreased expectedly (Fig. 2b). These results are in agreement with the pre-determined Pd to Pt atomic ratios in the synthesis. The Pt to Pd atomic ratio explored by XPS for the catalysts was tabulated in Table 1. Although deviations of nominal ratios from the ratios detected by XPS existed in all the catalysts, the general trend follows the same order. Surface segregation of Pt was found for the Pd_1Pt_1/C, Pd_2Pt_1/C and Pd_4Pt_1/C catalysts, on the contrary, surface rich of Pd was found for the Pd_6Pt_1/C catalyst.

Table 1
Comparison of the formic acid oxidation of the catalysts.

Catalyst name	Nominal Pd to Pt atomic ratio	Pd to Pt atomic ratio detected by XPS
Pd_1Pt_1/C	1:1	0.65:1
Pd_2Pt_1/C	2:1	1.91:1
Pd_4Pt_1/C	4:1	2.84:1
Pd_6Pt_1/C	6:1	6.98:1

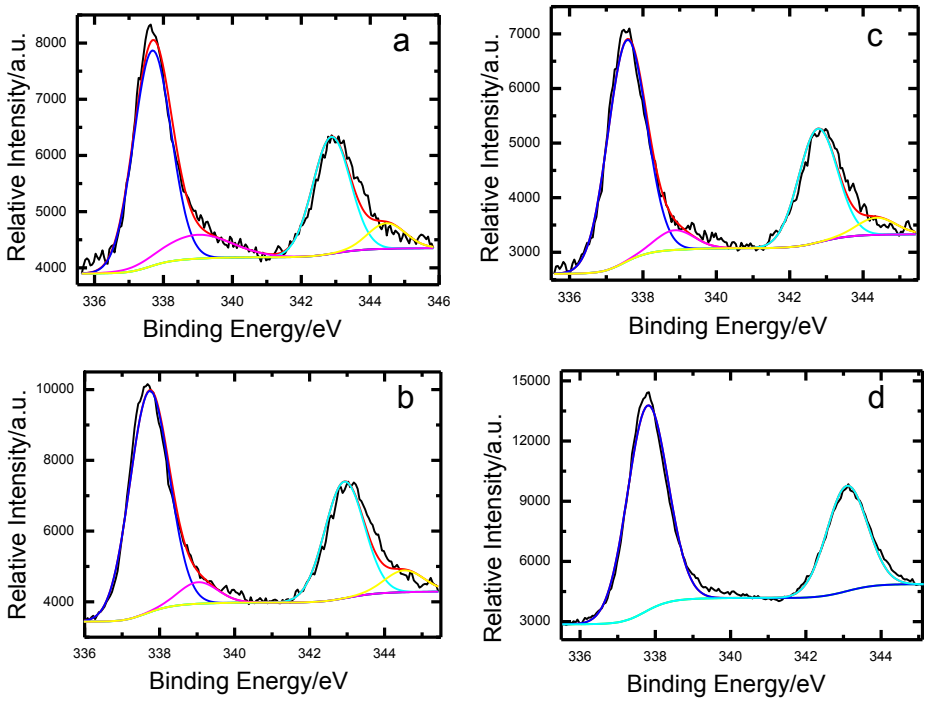

Fig. 3. Deconvolution of the Pd 3d spectra for the (a) Pd_1Pt_1/C catalyst (b) Pd_2Pt_1/C catalyst (c) Pd_4Pt_1/C catalyst and (d) Pd_6Pt_1/C catalyst.

The Pt 4f and Pd 3d spectra of Pt-C^{-1} in Fig. 2 were further deconvoluted into pairs of doublets, which are shown in Fig. 3 (for Pd 3d spectra) and Fig. 4 (for Pt 4f spectra), respectively. The Pd 3d spectra were deconvoluted into two pairs of doublets for the Pd_1Pt_1/C (Fig. 3a), Pd_2Pt_1/C (Fig. 3b) and Pd_4Pt_1/C (Fig. 3c) catalysts: the more intense doublet at 337.7 eV and 342.9 eV is a signature of metallic Pd and the less intense one at 338.8 eV and 344.4 eV is often assigned to oxidized Pd [12]. In comparison, only one pair of doublet contributed by metallic Pd was found for the Pd_6Pt_1/C (Fig. 3d). The Pt 4f spectra were deconvoluted into two pairs of doublets for the Pd_1Pt_1/C (Fig. 4a) and Pd_2Pt_1/C (Fig. 4b), respectively, whereas only one pair of metallic Pt doublet could be deconvoluted for the Pd_4Pt_1/C (Fig. 4c) and the Pd_4Pt_1/C (Fig. 4d) catalysts. Possible interactions between Pt and

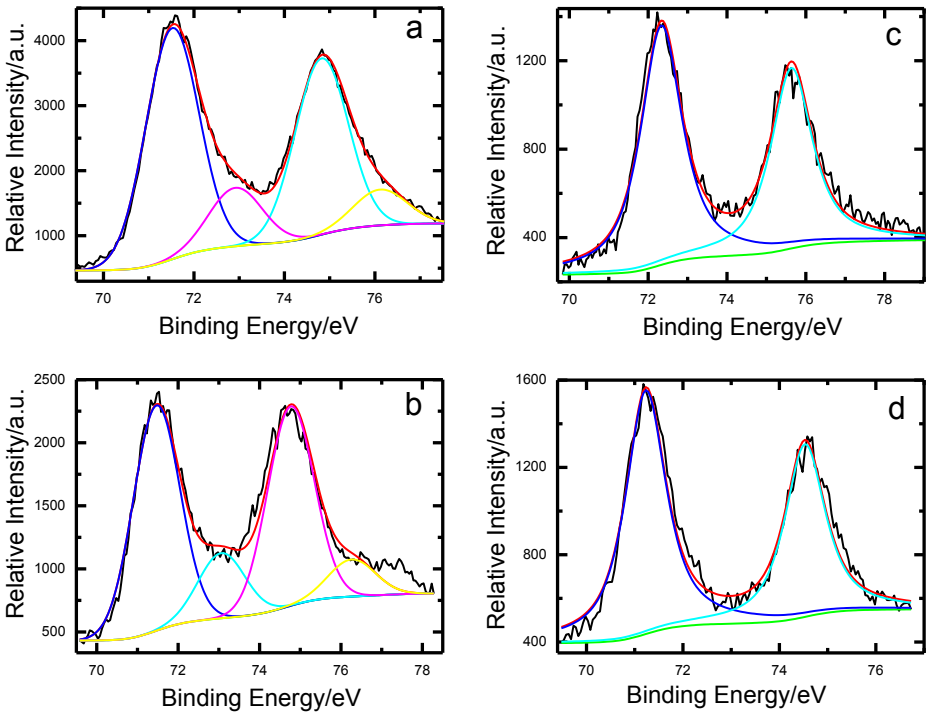

Fig. 4. Deconvolution of the Pt 4f spectra for the (a) Pd_1Pt_1/C catalyst (b) Pd_2Pt_1/C catalyst (c) Pd_4Pt_1/C catalyst and (d) Pd_6Pt_1/C catalyst.

Pd might have contributed to the differences in the oxidation states of Pd and Pt.

The CO stripping voltammograms of the catalysts are compared in Fig. 5a. To better illustrate the difference of the CO stripping pattern, a zoomed-in profile from potential of 0.4 V–0.8 V is depicted in Fig. 5b. It is commonly acknowledged that CO stripping is an effective electrochemical tool for the characterization of CO tolerance [21,25]. In general the voltammetric features agree well with the literature, in which CO oxidation went to completion in the first scan without any trace of CO in the second scan [19,26]. All the catalysts show dominant single CO stripping peak with various peak potentials. The CO stripping peak potential for Pt/C and Pd/C is at 0.55 V and 0.69 V, which lies in the lower and higher potential end on the potential scale, respectively. The CO stripping peak potential for Pd_1Pt_1/C, Pd_2Pt_1/C, Pd_4Pt_1/C and Pd_6Pt_1/C is at 0.60 V, 0.63 V, 0.66 V and 0.68 V, respectively, which is situated between that of Pd/C and Pt/C. The progressive decrease in the CO stripping peak potential with correspondingly decreased Pd amount is an indication of gradually increasing CO tolerance, which is somewhat expected since Pt alone catalysts perform better than Pd alone catalysts. The more negative shift of CO stripping peak implies the greater ease of CO removal and improved CO tolerance in practice. It should be noted that the CO stripping peak potential for Pd/C and Pd_6Pt_1/C is very close, probably ascribed to the surface Pd rich of the latter.

Since Pd is known to be an excellent hydrogen adsorption metal, the probing of the electrochemically active surface areas for Pd or Pd based electrocatalysts can only be carried out by CO oxidation.

Table 2
Comparison of the nominal ratio and that detected by XPS of the catalysts.

Catalyst	CO onset oxidation potential/V	Metal utilization efficiency/%	ECSA/$m^2\ g^{-1}$
Pt/C	0.55	96%	86.6
Pd_1Pt_1/C	0.60	94%	84.2
Pd_2Pt_1/C	0.63	89%	80.4
Pd_4Pt_1/C	0.66	86%	77.6
Pd_6Pt_1/C	0.68	84%	75.3
Pd/C	0.69	76%	68.3

The method assumes monolayer coverage of adsorbed CO and a CO to metal stoichiometry of 1:1 using a correspondence value of 420 μC cm^{-2} metal [27]. The ECSAs calculated by this way for the Pd/C and Pt/C is 68.3 and 86.6 $m^2\ g^{-1}$, respectively, whereas the ECSA of the rest catalyst is in between of these two values (Table 2). It can be seen that the addition of Pd to Pt could enhance the ECSA, i.e. dispersion of the catalysts. Assuming an average particle size of 3 nm and ideally spherical particles for all the catalysts prepared in this work, the surface area of purely geometry considerations could be calculated, according to ref. [28], to be 90 $m^2\ g^{-1}$. The metal utilization efficiency for the Pt/C and Pd/C catalyst, obtained by the percent of ECSA determined by CO oxidation over geometric surface area, is 96% and 76%, respectively, indicative of a very high dispersion of noble metals in this work. Table 2 summarized the CO onset oxidation potential, metal utilization efficiency and ECSAs of the catalysts.

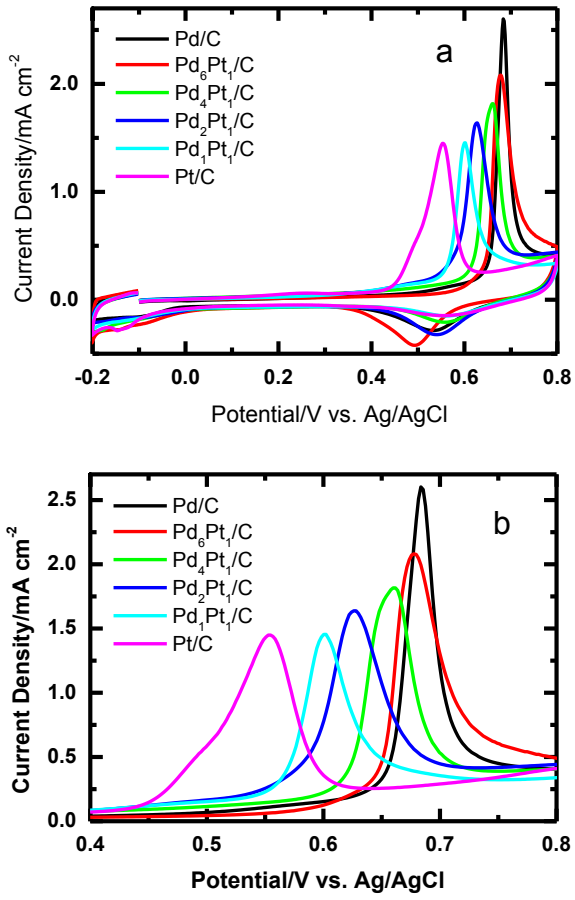

Fig. 5. CO stripping voltammograms in 0.5 M H_2SO_4 for the catalysts at room temperature (scan rate = 20 mV s^{-1}) (a) full profile and (b) zoomed-in profile.

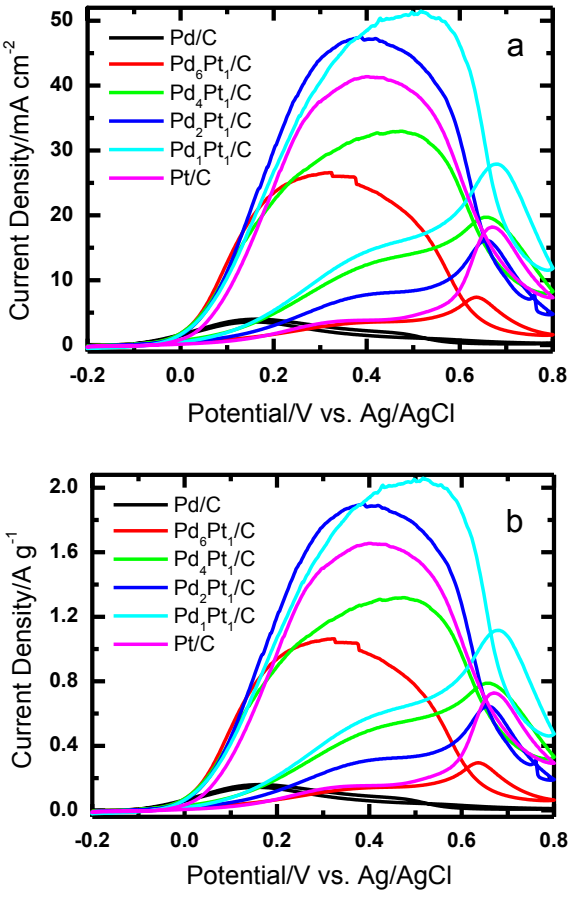

Fig. 6. Cyclic voltammograms of formic acid electrooxidation for the catalysts in 0.5 M HCHO+0.5 M H_2SO_4 measured at 20 mV s^{-1} at room temperature (a) normalized to the geometric surface area and (b) normalized to the total metal mass.

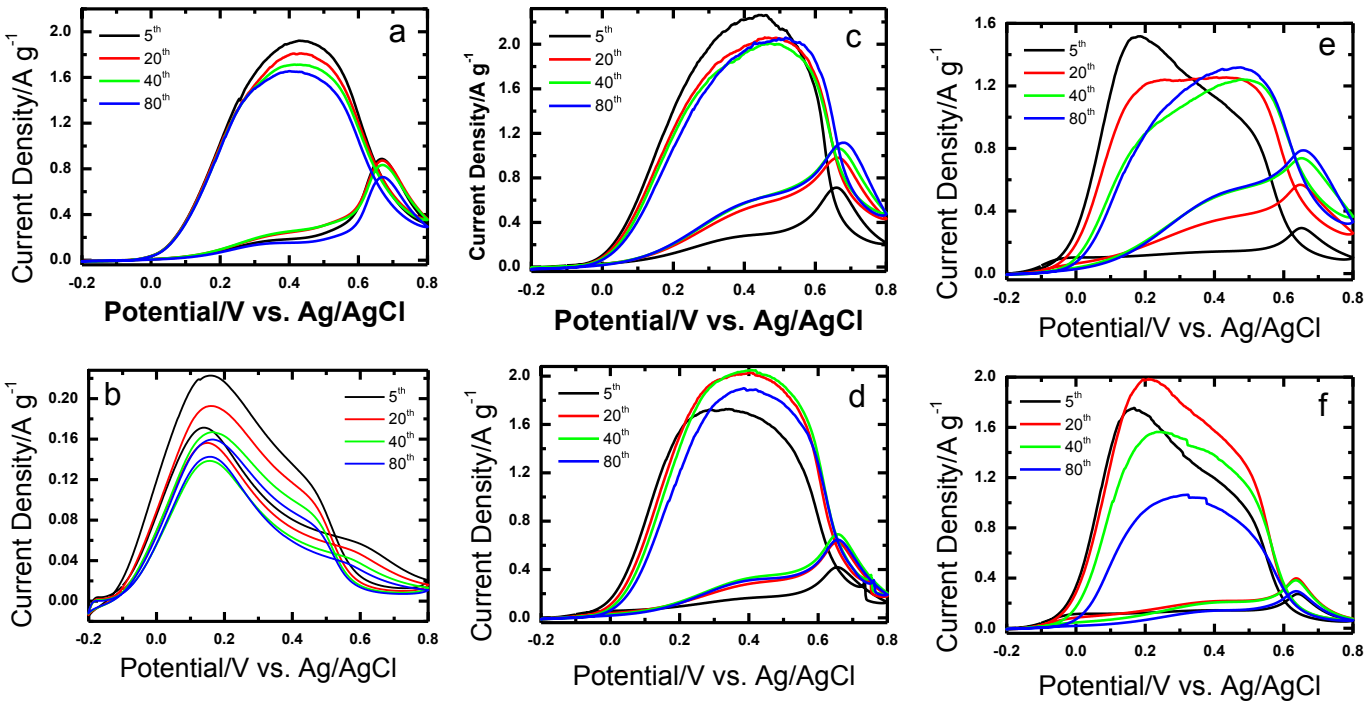

Fig. 7. Steady decay of formic acid electrooxidation for the catalysts at room temperature (the numbers in the figure indicate the scan number) (a) the Pt/C catalyst, (b) the Pd/C catalyst, (c) the Pd_1Pt_1/C catalyst (d) the Pd_2Pt_1/C catalyst (e) the Pd_4Pt_1/C catalyst and (f) the Pd_6Pt_1/C catalyst.

The formic acid electrooxidation on the catalysts in 0.5 M HCHO + 0.5 M H_2SO_4 at room temperature at a scan rate of 20 mV s^{-1} is shown in Fig. 6. The current density has been normalized to the geometric surface area of the electrode in Fig. 6a (0.196 cm^2) together with total metal loading in Fig. 4b and is an indication of mass-normalized current density. The forward and backward scan follows almost the same path for the Pd/C catalyst, indicative of direct pathway mechanism for formic acid oxidation on the Pd/C catalyst. The Pt/C catalyst, along with other Pt added catalysts (the Pd_1Pt_1/C, Pd_2Pt_1/C, Pd_4Pt_1/C and Pd_6Pt_1/C catalyst), shows a typical current hysteresis in the forward and backward scan and a peak current density at potential ~0.63 V during the positive potential patrol, which is typical of formic acid oxidation on Pt based catalysts. These commonly seen characteristics also confirmed an indirect pathway mechanism for Pt and Pt based catalysts even with low Pt loading (the Pt loading for the Pd_6Pt_1/C catalyst is as low as 4.7 wt.%). The onset formic oxidation for Pd/C and Pt/C is −0.13 V and −0.06 V, respectively, whereas the onset potential for Pd_xPt_y/C is in between of these two ends. It should be noted that the maximum mass-normalized activity in this work in the reverse scan is ~50 mA cm^{-2} (Fig. 6a), which is equal to 2 A mg^{-1} metal (Fig. 6b). In order to have a fair comparison with similar work in references, herein we listed some published results: for example, 20 mA cm^{-2} (0.5 M HCHO+0.5 M H_2SO_4, 50 mV s^{-1}) was reported in Refs. [16], 1.5 A mg^{-1} metal (0.5 M HCHO + 0.1 M H_2SO_4, 50 mV s^{-1}) in Refs. [10], 0.6 A mg^{-1} metal (0.5 M HCHO+0.1 M H_2SO_4, 50 mV s^{-1}) in Refs. [5], 1.1 A mg^{-1} metal (0.1 M HCHO + 0.1 M H_2SO_4, 10 mV s^{-1}) in Refs. [12], 0.55 A mg^{-1} metal (0.5 M HCHO + 0.5 M H_2SO_4, 50 mV s^{-1}) in Ref. [29]. It can be seen that our reported result in this work is the best amongst those published.

Fig. 7 recorded the steady decay of formic acid electrooxidation for the catalysts at room temperature. The catalysts were cycled in 0.5 M HCHO + 0.5 M H_2SO_4 at 20 mV s^{-1} for 80 scans and selected scans were recorded to investigate the catalyst stability. The decay rate for Pd/C and Pt/C, which is calculated by the peak current decrease in the reverse scan (from the 5th to the 80th scan), is 28% and 14%, respectively (Figs. 7a and b). The poor stability of the Pd/C catalyst was again confirmed in this work. With the increased cycling, the reverse scan evolved from a close-to-symmetric profile to a broadened plateau for all the Pd_xPt_y/C catalysts (Fig. 7c–f) and the onset formic acid oxidation potential moved positively with the most positive shift occurred on the Pd_6Pt_1/C catalyst (Fig. 7f). Whatsoever, the stability of the Pt added Pd_xPt_y/C catalyst is more or less enhanced relative to Pd alone one and this might be originated from the high dispersion of the noble metal catalysts and the absence of high molecular stabilizing agents prepared in this work.

4. Conclusions

A modified citrate reduction method assisted by inorganic stabilizers was used to prepare carbon supported Pd_xPt_y/C catalysts and tested out for formic acid electrooxidation. Highly dispersed catalysts were obtained with a citrate to metal precursor and KNO_3 stoichiometry of 1.5:1 and 15:1, respectively. The metal utilization efficiency was calculated to be from 84% for the Pd_6Pt_1/C catalyst to 94% for the Pd_1Pt_1/C catalyst, respectively. The formic acid oxidation activity and stability was found to be highly dependent on the Pd/Pt atomic ratio. The electrocatalytic ability of the resulting catalyst for formic acid was explored to exhibit striking mass-normalized activities compared with those from literature.

Acknowledgements

We would like to thank the Project on the Integration of Industry, Education and Research of Guangdong Province (2012B091100144), the Fundamental Research Funds for the Central Universities (2013ZZ0064) and Shanxi Province Science Foundation for Youths (No. 2012021006-1) for the financial supports of this work.

References

[1] X. Zhao, M. Yin, L. Ma, L. Liang, C.P. Liu, J.H. Liao, T.H. Lu, W. Xiong, Energy Environ. Sci. 4 (2011) 2736–2753.
[2] A. Serov, C. Kwak, Appl. Catal. B Environ. 90 (2009) 313–320.
[3] Y.Y. Shao, G.P. Yin, Z.B. Wang, Y.Z. Gao, J. Power Sources 167 (2007) 235–242.
[4] M.K. Debe, Nature 486 (2012) 43–51.
[5] B. Liu, H.Y. Li, L. Die, X.H. Zhang, Z. Fan, J.H. Chen, J. Power Sources 186 (2009) 62–66.
[6] S.M.M. Ehteshami, S.H. Chan, Electrochim. Acta 93 (2013) 334–345.
[7] P. Hong, F. Luo, S.J. Liao, J.H. Zeng, J. Power Sources 195 (2010) 7332–7337.
[8] N.V. Rees, R.G. Compton, J. Solid State Electrochem. 15 (2011) 2095–2100.
[9] Y.J. Kang, L. Qi, M. Li, R.E. Diaz, D. Su, R.R. Adzic, E. Stach, J. Li, ACS Nano 6 (2012) 2818–2825.
[10] J. Chai, F.H. Li, Y.W. Hu, Q.X. Zhang, D.X. Han, L. Niu, J. Mater. Chem. 21 (2011) 17922–17929.
[11] H.X. Zhang, C. Wang, J.Y. Wang, J.J. Zhai, W.B. Cai, J. Phys. Chem. C. 114 (2010) 6446–6451.
[12] E.A. Baranova, N. Miles, P.H.J. Mercier, Y. Le Page, B. Patarachao, Electrochim. Acta 55 (2010) 8182–8188.
[13] J.H. Wee, K.Y. Lee, J. Power Sources 157 (2006) 128–135.
[14] F. Maillard, G.Q. Lu, A. Wieckowski, U. Stimming, J. Phys. Chem. B 109 (2005) 16230–16243.
[15] A. Chen, P. Holt-Hindle, Chem. Rev. 110 (2010) 3767–3804.
[16] S. Zhang, Y.Y. Shao, G.P. Yin, Y.H. Lin, Angew. Chem. Int. Ed. 49 (2010) 2211–2214.
[17] R. Fabio, G.S. Gunther, K. Rudiger, W. Alexander, Angew. Chem. Int. Ed. 44 (2005) 2190–2209.
[18] N.V. Long, M. Ohtaki, T.D. Hien, J. Randy, M. Nogami, Electrochim. Acta 56 (2011) 9133–9143.
[19] L.G. Feng, F.Z. Si, S.K. Yao, W.W. Cai, W. Xiong, C.P. Liu, Catal. Commun. 12 (2011) 772–775.
[20] X. Li, I.M. Hsing, Electrochim. Acta 51 (2006) 3477–3483.
[21] T.Y. Jeon, S.J. Yoo, Y.Y. Cho, H.Y. Park, Y.E. Sung, Electrochem. Commun. 28 (2013) 114–117.
[22] P. Hong, S.J. Liao, J.H. Zeng, X.J. Huang, Int. J. Hydrogen Energy 36 (2011) 8515–8524.
[23] J.H. Zeng, M.J. Han, X.Y. Lu, D. Chen, S.J. Liao, Electrochim. Acta 112 (2013) 431–438.
[24] C.S. Lin, M.R. Khan, S.D. Lin, J. Coll. Interface Sci. 287 (2005) 366–369.
[25] L.G. Jose, T. Mikhail, S. Frode, S. Svein, M. Navaneethan, R. Magnus, C. De, G. Sergio, A. Selim, E. Bryan, J. Electroanal. Chem. 655 (2011) 140–146.
[26] Y.C. Hsieh, L.C. Chang, P.W. Wu, Y.M. Chang, J.F. Lee, Appl. Catal. B Environ. 103 (2011) 116–127.
[27] J.H. Zeng, J.Y. Lee, J.J. Chen, P.K. Shen, S.Q. Song, Fuel Cells 7 (2007) 285–290.
[28] F. Gloaguen, J.M. Leger, C. Lamy, J. Appl. Electrochem. 27 (1997) 1052–1060.
[29] S. Wang, X. Wang, S.P. Jiang, Phys. Chem. Chem. Phys. 13 (2011) 6883–6891.